BMC Biology

METHODOLOGY ARTICLE

Open Access

Modeling X chromosome inactivation using t5iLA naive human pluripotent stem cells

Yudan Shang[1†], Nannan Wang[2,3,4†], Haoyi Wang[2,3,4,5], Chenrui An[1*] and Wen Sun[2,3,5*]

Abstract

Background X chromosome inactivation (XCI) is a critical epigenetic event for dosage compensation of X-linked genes in female mammals, ensuring developmental stability. A robust in vitro model is required for mimicking XCI during the early stages of embryonic development. This methodology article introduces an advanced framework for the in-depth study of XCI using human pluripotent stem cells (hPSCs). By focusing on the transition between naive and primed pluripotent states, we highlight the role of long non-coding RNA X-inactive specific transcript (*XIST*) and epigenetic alterations in mediating XCI.

Results Our methodology enables the distinction between naive and primed hESCs based on *XIST* expression and the activity of X-linked reporters, facilitating the investigation of XCI initiation and maintenance. Through detailed experimental procedures, we demonstrate the utility of our hESC lines in modeling the process of human XCI, including the establishment of conditions for random XCI induction and the analysis of X chromosome reactivation.

Methods The study outlines a comprehensive approach for characterizing the X chromosome status in hPSCs, employing dual fluorescent reporter hESC lines. These reporter lines enable real-time tracking of XCI dynamics through differentiation processes. We detailed protocols for the induction of X chromosome reactivation and inactivation, as well as the X status characterization methods including cultivation of hESCs, flow cytometric analysis, RNA fluorescence in situ hybridization (FISH), and transcriptome sequencing, providing a step-by-step guide for researchers to investigate XCI mechanisms in vitro.

Conclusions This article provides a detailed, reproducible methodology for studying XCI mechanisms in vitro, employing hPSCs as a model system. It presents a significant advance in our ability to investigate XCI, offering potential applications in developmental biology, disease modeling, and regenerative medicine. By facilitating the study of XCI dynamics, this methodological framework paves the way for deeper understanding and manipulation of this fundamental biological process.

Keywords X chromosome inactivation, Human embryonic stem cells, Early embryogenesis

[†]Yudan Shang and Nannan Wang contributed equally to this work.

*Correspondence:
Chenrui An
an.chen.rui@163.com
Wen Sun
sunwen@ioz.ac.cn
Full list of author information is available at the end of the article

Background

XCI is a critical epigenetic event during early embryonic development in female mammals. This process involves the coordinated regulation of multiple genes at the transcriptional and epigenetic levels, leading to the random inactivation of one X chromosome and achieving dosage compensation for X-linked traits. The proper initiation, completion, and maintenance of XCI play crucial roles in embryonic development. Deviations from normal XCI processes can result in various XCI-related abnormalities, such as abnormal gene expression, skewed allelic inactivation, somatic reactivation of the X chromosome, and non-integer ploidy of sex chromosomes [1]. Currently, XCI is known to be regulated by *XIST*. In the initiation phase, XIST RNA envelops the X chromosome, recruits the polycomb repressive complexes (PRC1 and PRC2) [2–6], and associates with them, leading to the enrichment of ubiquitination of histone H2A [7, 8] and trimethylation at lysine 27 of histone 3 (H3K27Me3) [9]. The inactivated X chromosome then accumulates in the nucleolus, with histone H2A replaced by various macroH2A variants. Finally, promoter regions of the X chromosome undergo extensive methylation, resulting in the silencing of genes across the entire X chromosome [10, 11].

Over the past six decades of XCI research, most findings and conclusions have been derived from studies utilizing mice as the primary research model. However, the mechanisms governing XCI in mice may represent just one of several ways mammals regulate X chromosome dosage. In the 4–8 cell stage of female mouse embryos, the paternal X chromosome undergoes imprinted inactivation, persisting specifically in the trophectoderm cells of the extraembryonic tissue [12, 13]. Upon embryonic development to the blastocyst stage, inner cell mass cells reactivate both X chromosomes, erasing the Xist RNA coating and H3K27Me3 modification. Subsequently, during the embryo implantation stage, epiblast cells express Xist and initiate the random inactivation of one X chromosome. Mouse embryonic stem cells (mESCs) derived from the pre-implantation epiblasts maintain a naive pluripotent state. These cells possess two active X chromosomes, lack *Xist* expression, and can achieve random XCI upon differentiation [14, 15]. Therefore, both mouse pre-implantation epiblast and mESCs represent a state before XCI (pre-XCI), characterized by the absence of *Xist* expression.

In contrast to mice, no process of imprinted inactivation has been observed during early embryonic development in human female embryos. In the inner cell mass, both X chromosomes remain in an active state, with biallelic expression of *XIST* [16, 17]. Following implantation, one of the two X chromosomes undergo random inactivation [18]. In vitro, primed pluripotent human embryonic stem cells (hESCs) or human-induced pluripotent stem cells (hiPSCs) have mostly undergone XCI (post-XCI), and the X chromosome state is unstable [19–22]. Based on their X chromosome status, hPSCs were categorized into three classes [10]. Class I primed hPSCs obtain two active Xs with no *XIST* expression. Class II and III hPSCs both have undergone XCI. The inactive X of Class II primed hPSCs is coated with XIST, whereas almost no expression of *XIST* in Class III primed hPSCs, leading to exposing of the original inactive regions [10].

More importantly, the X chromosome state continues to be maintained post-differentiation [23–25]. Therefore, primed hPSCs cannot serve as suitable cellular models for studying XCI. Recently naive hESCs were established [26–34], some of which have demonstrated the reactivation of both X chromosomes [35–37]. However, most of these cells express *XIST* on only one X chromosome, inconsistent with the X chromosome state of human pre-implantation inner cell mass. Furthermore, these cells mostly fail to achieve random XCI post-differentiation [36, 38]. In our previous work, utilizing human embryonic stem cell lines carrying a tandem fluorescent reporter system for X chromosomes, we established naive hESCs with transcriptomes and X chromosome states consistent with human pre-implantation early embryos. Moreover, through staged differentiation, we successfully simulated the process of random XCI in vitro [39]. This paper provides a detailed description of the research methodology for in vitro modeling of human XCI.

Results

X chromosome status of conventional cultured primed hESCs

To dynamically monitor the X chromosome status of female hESCs, we utilized four primed pluripotent human embryonic stem cell lines, WIBR3^{MGT} and WIBR2^{MGT} with their original wildtype (WT) hESCs (WIBR3 and WIBR2). Both primed WIBR3^{MGT} and WIBR2^{MGT} featured a dual fluorescent reporter system on the X chromosome [38]. Through TALEN gene editing technology, GFP and tdTomato fluorescent reporter genes were individually inserted downstream of both alleles of the X chromosome gene *MECP2* in WIBR3 and WIBR2 hESCs with primed pluripotency, establishing the WIBR3^{MGT} and WIBR2^{MGT} cell lines [38–40] (Fig. 1A). In our previous work, we demonstrated that post-XCI primed WIBR3^{MGT} and WIBR2^{MGT} hESCs exhibited X-linked GFP-positive and tdTomato-negative status (single GFP positive, SG), while their pre-XCI primed hESCs were double positive (tdTomato and GFP positive, TG) (Fig. 1B, C) [39]. The following results took WIBR3^{MGT} as an example. The transcripts of *XIST* and

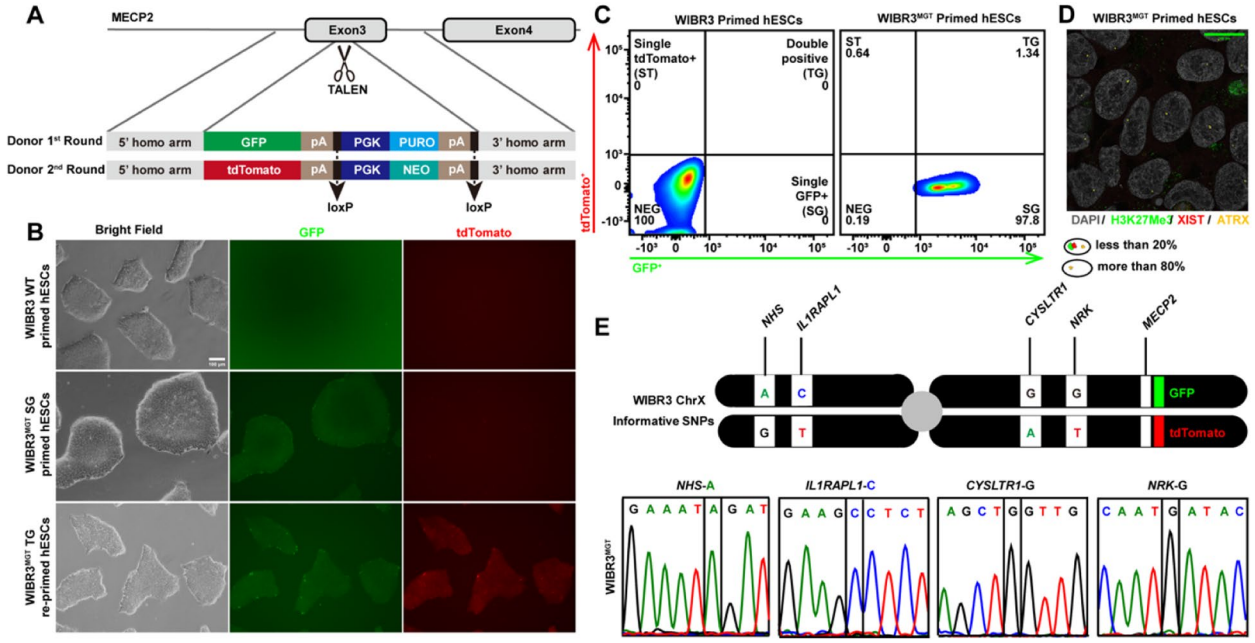

Fig. 1 Characterization of X chromosome status in initial primed hESCs. **A** strategy for generating WIBR3^{MGT} and WIBR2^{MGT} primed hESCs carrying a dual X-reporter system using TALEN-mediated gene editing. **B** Phase contrast and fluorescence images of WIBR3 WT (top panels) and post- (middle panels) and pre-XCI (bottom panels) WIBR3^{MGT} primed hESCs. Scale bar indicates 100 μm. **C** Flow cytometric analysis of the GFP and tdTomato expression in WIBR3^{MGT} primed hESCs. **D** Representative images of WIBR3^{MGT} primed hESCs maintained in E8 medium, analyzed by RNA-FISH to detect *XIST* (red) and *ATRX* (yellow) transcripts and by immunofluorescence co-staining of H3K27Me3 (green). Scale bar indicates 10 μm. **E** Upper panel: position of 4 predefined X-linked SNPs in WIBR3 [40]. Different colors represent different bases. Lower panel: sequencing peaks of 4 random SNPs in cDNA extracted from WIBR3^{MGT} cells. Panels **A** and **E** of this figure is adapted, with permission, from Ref.30© (2020) Cell Press

X-linked *ATRX* were stained by RNA FISH method, and co-stained with immunofluorescence of H3K27Me3. A punctate signal of ATRX could be detected in each nucleus of all cells (Fig. 1D), indicating that these conventional cultured primed hESCs contain an activated X chromosome. Approximately 20% of primed WIBR3^{MGT} hESCs detected colocalization of XIST cloud-like signal and H3K27Me3 signal in one cell nucleus (Fig. 1D). This shows that primed WIBR3^{MGT} hESCs have undergone XCI, and most cells have lost the ability to express XIST. We selected 4 single-nucleotide polymorphism (SNPs) on the X chromosome [40] (Fig. 1E). The cDNA sequencing results of reverse-transcribed mRNA showed that SNPs signals could only be detected on the GFP-labeled activated X chromosome (Fig. 1E).

X chromosome status of t5iLA naive hESCs

We applied the t5iLA naive pluripotency induction system [34, 38] to establish naive pluripotent embryonic stem cell lines. The following results took WIBR3^{MGT} t5iLA naive hESCs as an example. During the resetting, we observed two significantly different populations of double-positive cells: one group of cells with low expression of tdTomato (LT) and another group with high expression of tdTomato (HT) (Fig. 2A, B). For the WT t5iLA naive hESCs, we usually distinguished HT and LT cells based on their morphology, which HT naive cells exhibited more dome-shaped, whereas LT cells were more flat (Fig. 2C).

X chromosome status of sorted WIBR3^{MGT} HT and LT naive hESCs

The results of RNA-FISH showed that both HT and LT naive hESCs expressed ATRX and XACT on both X chromosomes. HT cells expressed biallelic XIST, while LT cells expressed monoallelic expression (Fig. 2D). The results of principal component analysis (PCA) showed that t5iLA HT naive hESCs were separated to primed hESCs, while LT naive hESCs were between HT naive and primed hESCs (Fig. 2E). By analyzing the SNPs sites on the X chromosome, it was found that after t5iLA induction, SNPs signals spanning the entire chromosome can be detected on both X chromosomes of HT and LT cells (Fig. 2F), further confirming that the two X chromosomes are active.

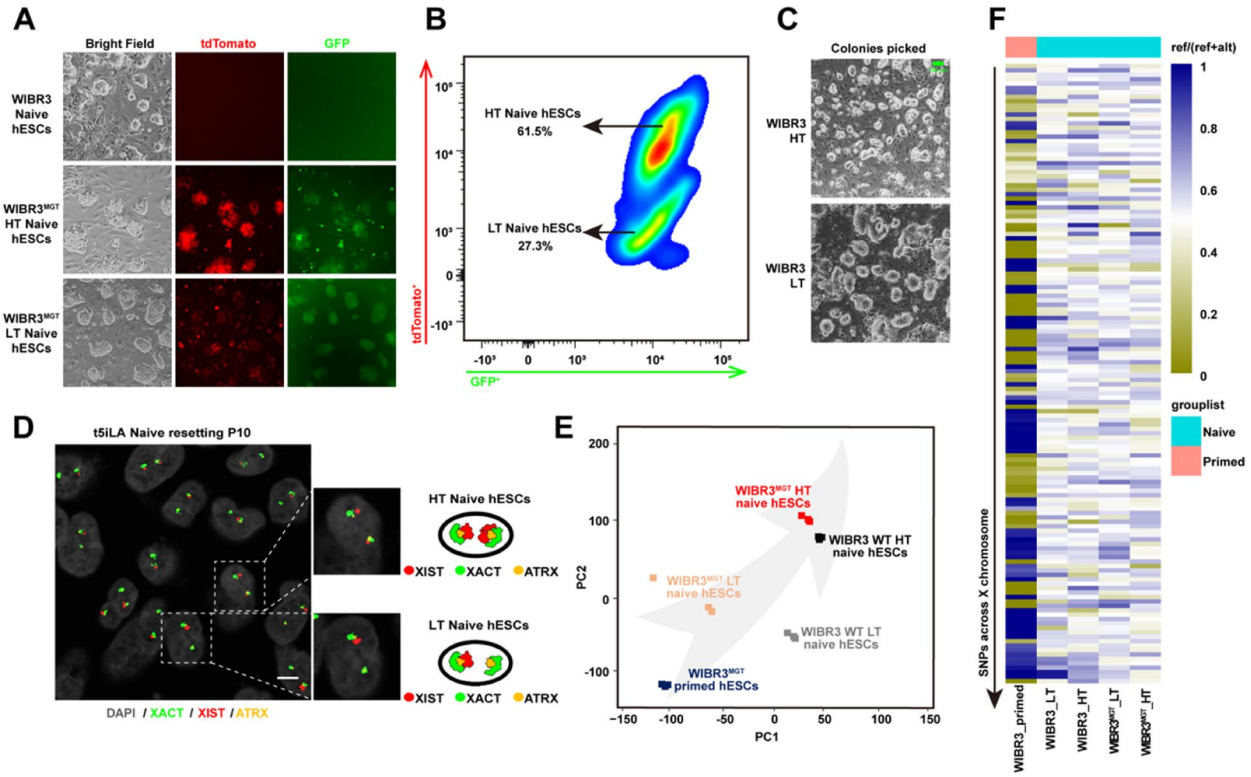

Fig. 2 Characterization of X Status of t5iLA naive hESCs. **A** Phase contrast and fluorescence images of WIBR3^{MGT} HT and LT t5iLA and WT naive hESCs. **B** flow cytometric analysis of the GFP and tdTomato expression at P10 of WIBR3^{MGT} t5iLA resetting. **C** Representative images of WIBR3 HT and LT t5iLA naive hESCs. Scale bar indicates 100 μm. **D** Left panel: representative RNA-FISH images of WIBR3^{MGT} t5iLA HT and LT naive hESCs, detecting *XACT* (green), *XIST* (red), and *ATRX* (yellow) transcripts. Right panel: cartoons of the HT and LT naive hESCs having different RNA FISH patterns. **E** PCA analysis of RNA-seq data from WIBR3^{MGT} primed hESCs, LT and HT naive hESCs derived from WIBR3^{MGT} or WIBR3. Every single dot represents one sample in each cell line. **F** Heatmap of allelic expression of X-linked genes in WIBR3 and WIBR3^{MGT} naive and primed hESCs, based on reads covering X-linked SNPs

Detection of XCI in t5iLA naive hESCs through teratoma formation in vivo

We induced differentiation by subcutaneously injecting t5iLA HT naive hESCs into NOD mice (Fig. 3A). The formed teratomas were identified by immunohistochemistry and could significantly distinguish cells of the three germ layer lineages, thus proving the differentiation potential of t5iLA HT naive hESCs (Fig. 3A). The isolated teratomas were then digested into single cells, and flow cytometry analysis revealed that 80% of the cells expressed only one fluorescent reporter gene on the X chromosome and both single GFP (SG) or tdTomato (ST) positive cells were detected, whereas the proportion of SG and ST cells was unbalanced (Fig. 3B). Next, we detected the X status of teratoma cells through XIST and ATRX RNA FISH and H3K27Me3 immunofluorescence co-staining. Among them, both most cells have monoallelic expression of XIST on the X chromosome and co-localize with enriched H3K27Me3, while a single ATRX signal is separated from it, confirming that these two groups of cells exhibit a complete XCI state. In contrast, a small proportion of cells only had two ATRX signals and no *XIST* expression or H3K27Me3 enrichment (Fig. 3C), indicating that after teratoma formation, most cells underwent XCI, and each chromosome has a chance to be selected to be inactive or remain active. The failure of a small proportion of cells to complete XCI may be due to differentiation that differs from development in vivo.

Detection of XCI in t5iLA naive hESCs through re-priming in vitro

Previous studies have shown that after mESCs (naive pluripotency) differentiate into mEpiSCs (mouse epiblast stem cells, mEpiSCs, primed pluripotency), all cells will undergo XCI [41]. The following results took WIBR3^{MGT} t5iLA naive hESCs as an example. We transferred WIBR3^{MGT} t5iLA HT naive hESCs back into the primed pluripotent culture system to induce differentiation (re-priming). It was found that after 5 days of differentiation, we detected SG, ST, and TG re-primed hESCs (Fig. 4A, B). The results of RNA FISH showed that about half of the re-primed hESCs displayed a co-localized signal of

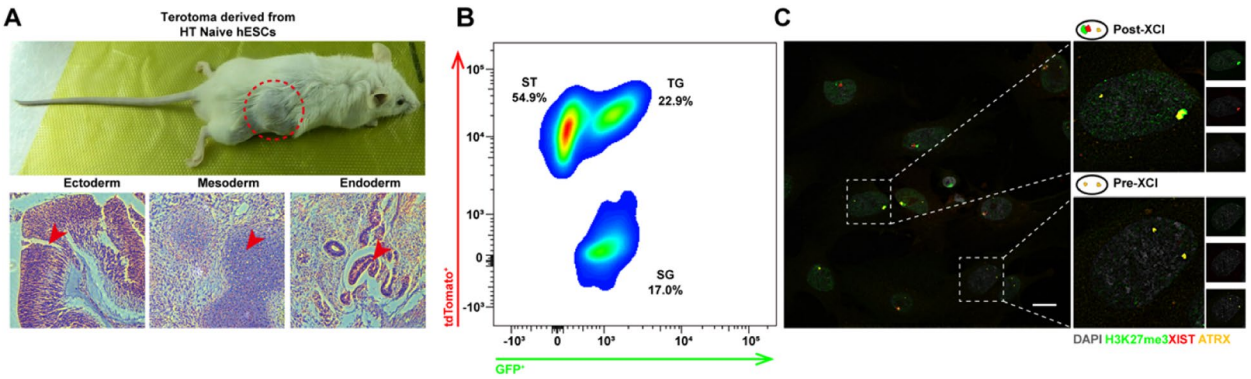

Fig. 3 Inducing XCI in t5iLA naive hESCs through teratoma formation in vivo. **A** Upper panel: representative image of the mouse carring terotoma (red circled). Lower panel: representative images of WIBR3^{MGT} HT naive hESCs teratoma shows differentiation of three germ layers by immunohistochemistry. Red arrows point respiratory epithelial tissue in endoderm, cartilage tissue in mesoderm and neuroepithelial tissue in ectoderm. **B** Histogram showing the single GFP (SG, in green), single tdTomato (ST, in red) and double positive (TG, in yellow) populations of teratoma cells differentiated from WIBR3^{MGT} HT naive hESCs. **C** Representative images of the teratoma cells, analyzed by RNA-FISH to detect XIST (red) and ATRX (yellow) expression with immunofluorescence co-staining of H3K27Me3 (green). Scale bar indicates 30 μm

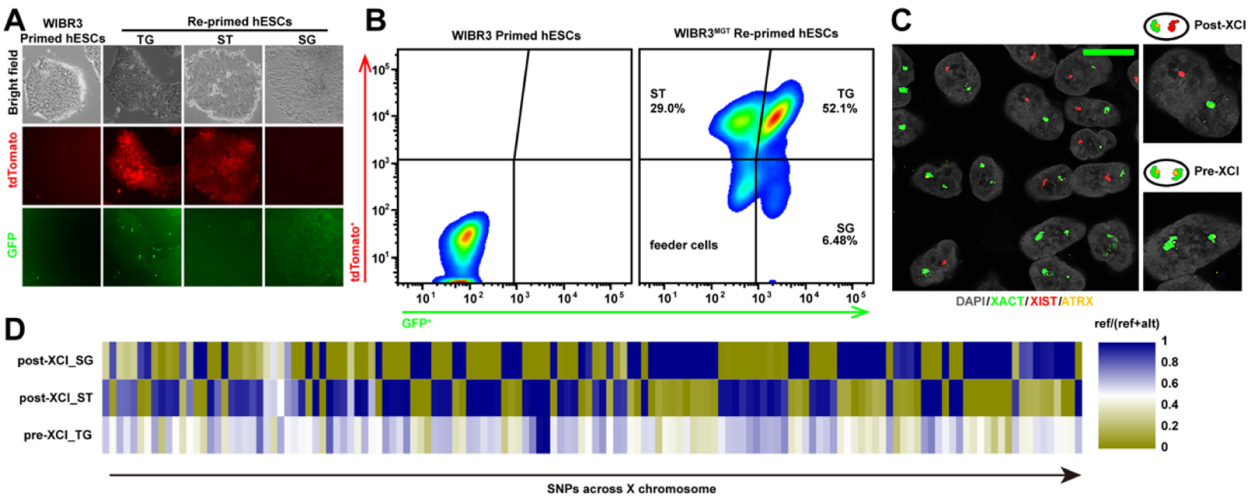

Fig. 4 Inducing XCI in t5iLA naive hESCs through re-priming in vitro. **A** Phase contrast and fluorescence images of repriming WIBR3^{MGT} HT naive hESCs at day 5. **B** Histograms showing the distribution of single GFP (SG, in green), single tdTomato (ST, in red), and double positive (TG, in yellow) hESCs re-primed from WIBR3^{MGT} 5iLA HT naive hESCs, by flow cytometric analysis. **C** Examples of WIBR3^{MGT} re-primed hESCs analyzed by RNA-FISH to detect XIST (red), XACT (green), and ATRX (yellow) expression. Scale bar indicates 10 μm. **D** Heatmap of allelic expressing X-linked SNPs in above samples, based on reads covering indicated SNPs

ATRX and XACT in each nucleus, and a separate XIST signal (Fig. 4C), indicating that these cells completed XCI. However, the other half of the re-primed hESCs possess two co-localization signals of ATRX and XACT, and neither the expression of XIST nor the enrichment of H3K27Me3 was detected (Fig. 4C, D), indicating that the two X chromosomes are still activated. The SNPs signal analysis results showed that the X-linkedSNP signals of the two FACs sorted post-XCI primed hESCs closely corresponded to the activities of the reporter genes they carried, indicating that the entire X chromosome was completely silenced after differentiation (Fig. 4E). In contrast, the sorted TG primed hESCs have SNPs signals covering the entire chromosome on both X chromosomes (Fig. 4D).

Random XCI through embryoid body differentiation into fibroblasts

We differentiated pre-XCI re-primed hESCs into fibroblasts by forming embryoid bodies (EBs) (Fig. 5A). Typically, the fibroblasts grow out of the attached EBs after two days (Fig. 5A). The results of flow cytometry analysis

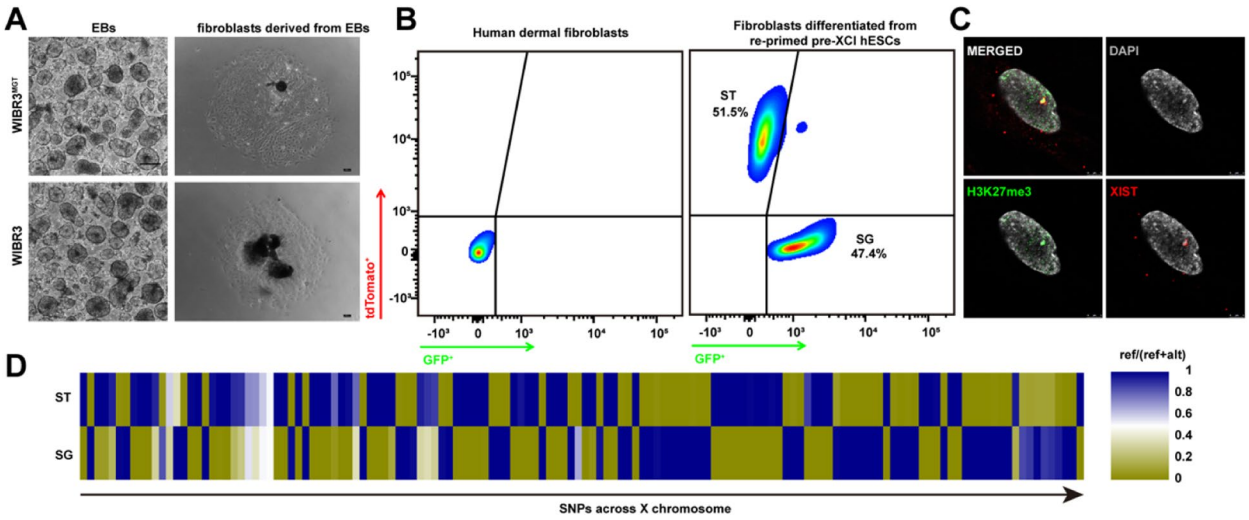

Fig. 5 Random XCI through embryoid body differentiation into fibroblasts. **A** Representative images of EBs (left panel) and fibroblasts (right panel) derived from pre-XCI WIBR3^{MGT} re-primed hESCs. Scale bar indicates 100 µm. **B** Flow cytometric analysis showing the distribution of GFP and tdTomato-positive fibroblasts derived from pre-XCI WIBR3^{MGT} re-primed hESCs through EB differentiation. Histograms reporting the proportions of single GFP (SG, in green), single tdTomato (ST, in red) and double positive (TG, in orange) cells. **C** Using differentiated fibroblasts in **B**, expression of XIST (red) and H3K27Me3 enrichment (green) are analyzed by RNA-FISH and immunofluorescence co-staining. **D** Heatmap of allelic expressing X-linked SNPs in SG and ST fibroblasts, based on reads covering indicated SNPs

of three biological replicates showed that all fibroblasts were single positive, and the proportions of ST and SG fibroblasts were similar, indicating that after this differentiation process, cells underwent almost completely random XCI (Fig. 5B). Furthermore, the results of RNA FISH of XIST and immunofluorescence co-staining of H3K27Me3 showed that all ST and SG fibroblasts exhibited co-localization of XIST and H3K27Me3 signals on a single inactivated X chromosome (Fig. 5C). Using RNA-Seq data of SG and ST fibroblasts, by analyzing SNPs across the X chromosome, it was found that in the two cells, corresponding SNP signals were only detected on the X chromosome activated by the fluorescent reporter gene, while the inactivated X chromosome was complete silenced (Fig. 5D).

Discussion

Most hESCs, derived from pre-implantation blastocysts, exhibit post-implantation epiblast molecular properties with XCI characteristics, hindering their utility in studying human X chromosome repression events [18]. Recent advancements in culture conditions have enabled the reversion of primed hESCs to a naive pluripotent state for modeling pre-implantation development, revealing heterogeneity in XCI among naive hESC populations [36, 37]. Two subpopulations, HT and LT, displayed distinct X chromosome activities, reminiscent of human pre-implantation epiblasts [17, 37]. HT cells exhibited bi-allelic XIST expression, in contrast to mono-allelic expression in LT cells. Despite previous reports, re-priming of HT naive hESCs resulted in XCI in 60% of cells in vitro and in vivo, and single GFP and tdTomato positive cells were both detected, whereas the proportions of these two types of cells were unbalanced. These findings challenged the existing understandings [36, 38]. In vitro differentiation protocols significantly impacted XCI outcomes, suggesting unknown mechanisms at play. The nascent field of human naive pluripotency, while advancing reprogramming techniques, faces the challenge of benchmarking against in vitro-generated human embryos [42]. The study's workflow offers insights into refining culture conditions for maintaining homogeneous naive pluripotency, a crucial step in modeling early human development. The asynchronous establishment of XCI in humans, accommodated by primed pluripotency in vitro, underscores the need for further investigation into the in vivo relevance of these findings [43]. The proposed reporter system holds promise in shedding light on the intricate dynamics of human XCI.

Conclusions

The establishment of naive hESCs and their successful modeling of XCI through various methodologies, including teratoma formation in vivo and stepwise differentiation in vitro, represent X status during early embryo development. The observed heterogeneity in XCI outcomes among naive hESC subpopulations, along with the proposed reporter system's potential, highlights the

evolving landscape of naive pluripotency research and emphasizes the need for further exploration of in vivo implications.

Methods

Workflow of monitoring human XCI in vitro

This study provides a comprehensive set of protocols for simulating human XCI in vitro using pluripotent stem cells (Fig. 6). The workflow is divided into two main parts: inducing X chromosome reactivation and inactivation. The assays for inducing to reactivate the X chromosome includes the establishment of human naive pluripotency and cultivation of hPSCs; the assays for inducing XCI includes re-priming, teratoma formation, EB formation, and fibroblast culture. The detailed methods for each type of cell culture and cell state transition were described below. As it is necessary to characterize the X chromosome status of the cells obtained at every

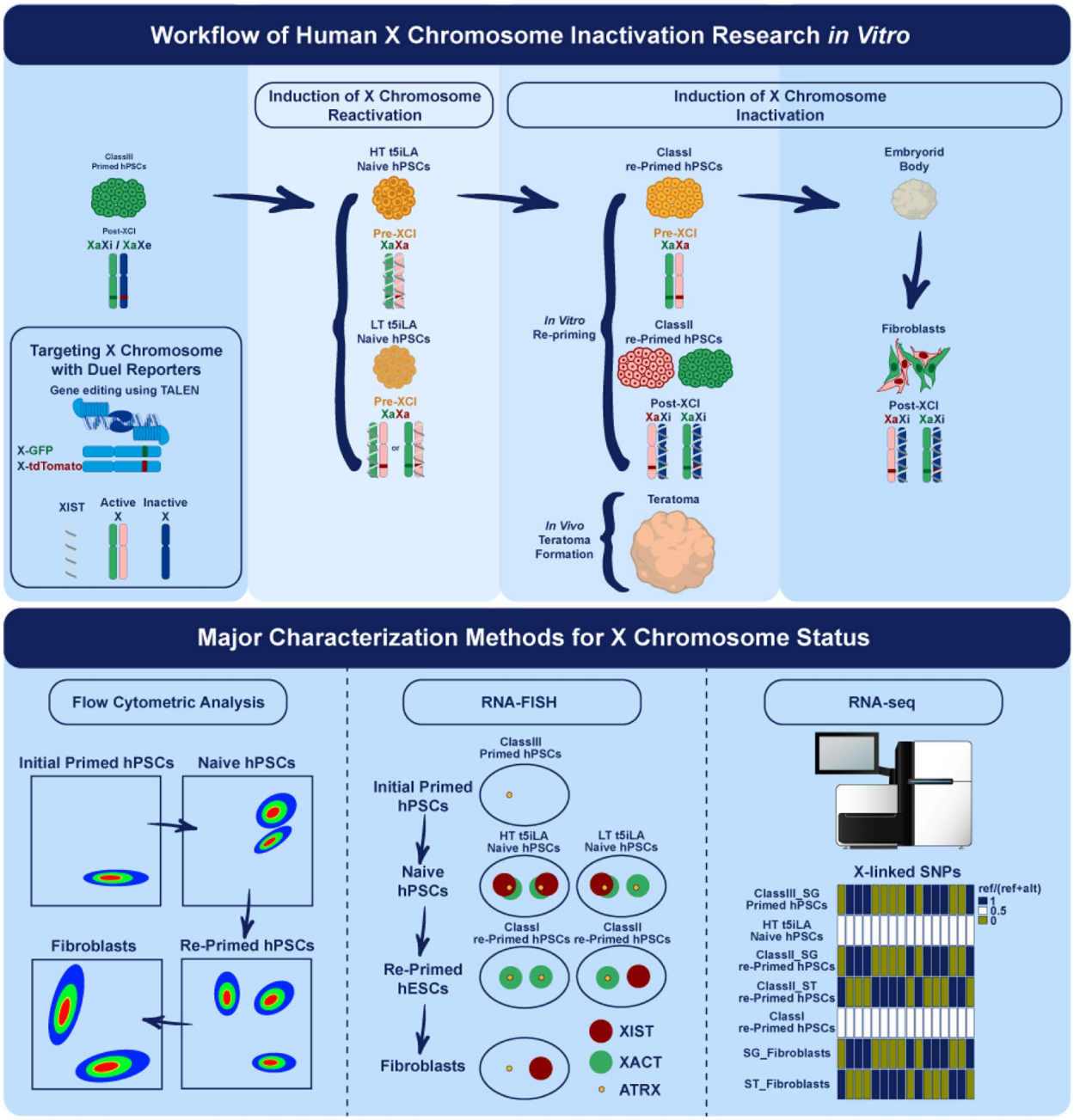

Fig. 6 Workflow of human XCI research in vitro

step of the above research workflow. We also detailed the characterization methods, which primarily include flow cytometry analysis or sorting, RNA-FISH, and analysis of X status based on RNA-seq data. The detailed methods for each technical approach are introduced in the following sections.

Induction of X chromosome reactivation

Establishment of human naive pluripotency

We followed the t5iLA naive resetting procedure based on our previous work. The culture medium and relevant biological reagents used in the experiments are detailed in Additional file: Table S1, and the recipes of media are listed in Additional file: Table S2.

Primed hESCs were first dissociated into single cells using Accutase. After 5 min, the cells were resuspended in E8 medium supplemented with Y27632 (10 μM) and counted. After centrifugation at 800 rpm for 5 min, the supernatant was removed. Cells were resuspended in human embryonic stem cells media (HESM) supplemented with Y27632 (10 μM) and plated on a pre-seeded feeder layer. Approximately $3–5\times10^5$ cells were plated per well in a six-well plate (exact cell numbers varied depending on the tolerance of different cell lines to the naive culture medium). The cells were cultured at 37℃, 5% O_2, 5% CO_2. After 1 to 2 days of recovery, the medium was switched to t5iLA medium [34]. Significant cell death may be observed at the initiation of induction. Fresh medium was replaced daily. Typically, after the third passage, $WIBR3^{MGT}$ and $WIBR2^{MGT}$ naive colonies could be enriched through fluorescence-activated cell sorting. Naive hESCs were passaged every 3 to 5 days using Accutase for single-cell dissociation.

Cultivation of hPSCs

Primed or re-primed hPSCs were cultured on Matrigel at 37 °C, 5% CO_2 using commercialized E8 medium. Cells were passaged at a ratio of 1:3 to 1:6 every 3–5 days. For passaging in a 6-well plate, cells were washed once with Ca^{2+}- and Mg^{2+}-free DPBS, then 1 mL of warmed 0.5 mM EDTA was added per well and incubated at 37 °C for 5 min. Subsequently, after gentle removal of EDTA, 1–2 mL of fresh E8 medium was added. The cells were then dissociated by gently pipetting 3–5 times with a 5-mL pipette to ensure complete detachment. The cells were transferred to a 15-mL centrifuge tube, then centrifuged at 600 rpm for 5 min. Following centrifugation, the supernatant was carefully aspirated, and fresh E8 medium was added. Subsequently, the cells were seeded onto Matrigel pre-coated dishes and allowed to adhere for a minimum of 1 h prior to daily media replacement. The culture medium was detailed in the Additional file: Table S2.

Induction of X chromosome inactivation

Re-priming of naive hPSCs in vitro

For naive-to-primed pluripotency differentiation (re-priming), naive hESCs were digested with Accutase and counted. Subsequently, 5×10^5 cells were plated in each well of a six-well plate and reseeded onto a feeder layer. The medium directly used was HESM supplemented with Y27632. The next day, Y27632 was removed, and the medium was replaced. After 5 days of induction, re-primed hESCs were washed once with pre-warmed DMEM/F12. Each well was then treated with 1 mL of 1 mg/mL Collagenase Type IV for digestion. After 20 min, the edges of flattened re-primed hESC clones curled up visibly. Cells were scraped off the culture plate using a cell scraper, transferred to a 15-mL centrifuge tube, and allowed to settle by gravity. After 5 min, the supernatant was carefully removed, leaving approximately 1 mL of cell suspension. Subsequently, 4 mL of HESM was added for resuspension, followed by a further 5-min incubation. After removing the supernatant, cells were resuspended in E8 medium supplemented with Y27632 and seeded onto Matrigel for expansion.

Teratoma formation in vivo

To promote teratoma formation and differentiation, we resuspended digested $WIBR3^{MGT}$ naive hESCs in 250 μL of Matrigel at 4 ℃. Subsequently, 1.0×10^6 cells were injected on opposite sides of the dorsal region of each immunodeficient mouse. Approximately 8 weeks later, when teratomas reached a diameter of 3 cm, mice were euthanized. Each isolated teratoma was cut into two halves. Then half of each terotoma was fixed in formalin, embedded in paraffin, and sectioned. Prepared sections were stained with hematoxylin and eosin for observation under a microscope, enabling the discrimination of three germ layers. The remaining half of each teratoma was immediately digested with 0.25% Trypsin–EDTA for 5 min, followed by flow cytometric analysis. The cell processing method for flow cytometric analysis is referenced from section above.

Embryoid body formation and differentiation into fibroblasts

To differentiate into fibroblasts using embryoid body differentiation, Class I re-primed hESCs were digested into single cells using Accutase. After centrifugation at 800 rpm for 5 min, hESCs were resuspended in fibroblast culture medium (Additional file: Table S3) supplemented with 10 μM Y27632. The amount of resuspension medium was calculated based on a ratio of 5×10^5 Class I re-primed hESCs per 30 μL, containing added Y27632. Subsequently, 30 μL drops were evenly pipetted onto the lids of 100-mm culture dishes. Next, 15 mL of fibroblast culture medium was added to the dishes, and the

prepared lids were carefully inverted onto the dishes. After 5 days, multiple embryoid bodies formed in each droplet. The entire content was washed down with fibroblast culture medium and seeded onto a new 100-mm culture dish pre-coated with gelatin. Fresh medium was exchanged every 2 days, and the entire differentiation process lasted approximately 3 to 5 days.

Major characterization methods for X chromosome status

Flow cytometric analysis and sorting

Cells were analyzed when confluency reached at least 50%. Cells were washed once with DPBS, followed by the addition of 1 mL of pre-warmed Accutase, with subsequent incubation at 37 °C for 5 min. Then gentle pipetting with a 1-mL pipette was employed, followed by the addition of 2 mL of E8 or t5iLA medium supplemented with 10 μM Y27632. Upon thorough mixing and removal of cell clumbs, the cells were passed through a 40-μm filter to obtain a homohenous single-cell suspension. This suspension was then transferred to a 15-mL centrifuge tube, centrifuged at 800 rpm for 3 min, and the supernatant was carefully decanted. Subsequently, the cell pellet was resuspended in 0.5–1 mL of DPBS containing 5% FBS and maintained on ice. The resulting digested single-cell suspension underwent analysis using the LSR II SORP flow cytometer (Beckton-Dickinson). Excitation was achieved using a yellow/green laser (561 nm, 25 mW), while detection utilized a 610/20 bandpass filter for Cy3. Additionally, a blue laser (Sapphire Solid State 488 nm, 100 mW) was utilized for excitation, with detection employing a 525/50 bandpass filter for Green Fluorescent Protein (GFP). Flow cytometry data analysis was conducted using Flowjo software (v10.0.7).

Preparation of RNA-FISH probes

This study utilized a reported RNA FISH probe preparation method [44]. The homemade XIST probe was derived from the first exon of the XIST gene (GenBank U80460: 61251–69449), while the XACT probe was derived from the BAC integrating XACT (RP11-35D3, BACPAC). Both XIST and XACT DNA probes were labeled with Cy3-dUTP or FITC-dUTP using the Nick Translation Kit. The reaction system is listed in Additional file: Table S3.

We added 2 μg XIST and XACT DNA in the above reaction system, and underwent a 2 h reaction at 15 °C in a PCR instrument, followed by a 15-min reaction at 65 °C. Subsequently, 2 μg (2 μL) Cot-1 DNA and 40 μg (4 μL) of fish sperm DNA were added to each reaction system, followed by the addition of 1/10 volume of 2.6 μL Na-Acetate and 52 μL of ethanol. The mixture was then cooled at − 20 °C for 30 min, followed by centrifugation at 16,000 *g*, 4 °C for 30 min. The supernatant was removed, and the precipitated probe DNA was air-dried. The probe was dissolved in hybridization buffer using 100 μL to achieve a final concentration of 20 ng/μL. Finally, the probe was aliquoted, protected from light, and stored at − 20 °C. The ATRX RNA-FISH probe was purchased from Stellaris.

RNA-FISH

This study employed a well-established RNA FISH method [44]. Firstly, 75% ethanol immersed glass coverslips were placed in a culture dish and coated with feeder cells or Matrigel. Naive, primed or re-primed hESCs, teratoma cells as well as fibroblasts, were passaged at least three generations in vitro before detection. After aspirating the supernatant, cells were washed once with DPBS and then digested with Accutase to single cells, which were then seeded onto feeder cells or Matrigel-coated plates.

Once cell confluence reached above 60%, the supernatant was removed, and the cells were air-dried for 5 min. Subsequently, cold DPBS was added and allowed to stand for 5 min. After removal, cold CSK-T was added for a 3-min membrane permeabilization treatment. Then, the supernatant was aspirated, and 4% paraformaldehyde was added for a 10-min fixation. The coverslip with cells was picked up using a syringe needle, sequentially soaked in 70%-80%-90%-100% ethanol for 5 min each during dehydration, and the probes were denatured at 80 °C for 10 min during this period. The coverslip was then rapidly transferred to a pre-heated 42 °C hybridization chamber, and pre-annealed for 5 to 60 min (exact time determined by the required dehydration time). Meanwhile, the hybridization reaction container was prepared. A 100-mm culture dish was prepared, three layers of DEPC water-soaked paper towels were placed on the dish, and the sealed film was placed on the paper towels.

After dehydration, the coverslip with cells was air-dried. Then, approximately 100 μL of hybridization fluid containing the probe was added dropwise to the sealed film, and the coverslip with cells was inverted onto the hybridization buffer. The 100-mm culture dish was tightly sealed with the sealed film. Then, it was placed in a hybridization oven preheated to 42 °C for 12 to 16 h.

Before collecting the coverslip after hybridization, 2 × SSC-50% formamide and 2 × SSC were preheated to 45 °C. The coverslip was taken out, washed three times with 2 × SSC-50% formamide, and then washed three times with 2 × SSC, each time for 5 min. Finally, approximately 10 μL of DAPI-containing anti-quenching mounting solution was added to the slide. The coverslip with cells was then placed on the mounting solution. After drying, images were captured using

a Leica TCS SP8 laser confocal microscope, equipped with various filters for DAPI, Cy3, Cy5, and FITC.

RNA-seq for identifying X chromosome status

To prepare RNA-Seq samples, 1.0×10^6 naive or primed hESCs were treated with Trizol to extract total RNA. Paired-end sequencing reactions with 150-bp reads were performed on an Illumina X Ten sequencer. All sequencing data were aligned to the UCSC human genome annotation (hg19) using Hisat2 (2.1.0) and Cufflinks (2.2.1) software under default settings. Reads with FPKM (fragments per kilobase of transcript per million mapped reads) values not less than 1 and with unique genome positions were used in subsequent analyses. Principal component analysis and clustering analysis were performed using prcomp and pheatmap in R, respectively.

The SNP annotation file (dbSNP151) was used to identify X chromosome allelic-specific expression. Additionally, SNP sites used in the analysis were detected in at least one sample. Based on previous research on human pre-implantation embryos [17], the analysis method for overall expression levels of X chromosome genes involved a sliding window of 50 genes, and the selected genes had FPKM values not less than 1 in all samples. Previous RNA-FISH and RNA-seq analyses confirmed that HT naive hESCs exhibited activation of both X chromosomes with biallelic expression of XIST, consistent with the X chromosome status of the human pre-implantation epiblast. In contrast, LT naive hESCs, although also exhibiting biallelic activation of both X chromosomes, expressed XIST on only one X chromosome. Consequently, HT naive hESCs were used for subsequent simulation of human XCI.

Immunofluorescence staining

Following DPBS washing, cells underwent membrane permeabilization using CSK-T, followed by fixation with 4% paraformaldehyde. Blocking solution was applied for 20 min. Primary antibodies (1:500) diluted in FBS were added, and the cells were incubated overnight at 4℃. After three 5-min washes with washing solution, secondary antibodies (1:1000) were added, and cells were incubated at 37℃ in the dark for 1 h. Subsequently, cells were washed three times for 5 min each with washing solution. Finally, cells were mounted using anti-fade mounting medium with DAPI. Images were captured using a Leica TCS Sp8 laser scanning confocal microscope, and data were processed using ImageJ (1.47 V) software. For a comprehensive list of antibodies, see Additional file: Table S4.

Identification of dedfined X-linked SNPs

In this study, the genomic information obtained from WIBR3 hESCs, as detected by the Affymetrix human SNP array 6.0, was analyzed [40]. The array intensity data and SNP information were extracted using Affymetrix Genotyping Console (v4.20) software. Cell samples were lysed, and total RNA was extracted using Trizol. cDNA was synthesized using the TransScript One-Step gDNA Removal and cDNA Synthesis SuperMix kit. Subsequently, approximately 500-bp fragments containing SNP sites were amplified using AccuPrime Taq DNA polymerase. The PCR products were then ligated to the T vector using the pEASY-T1 Cloning Kit, followed by transformation into DH5α *E. coli* on plates. After 16 h, 15 to 20 individual clones were selected and sequenced. By calculating the number of different clones, the distinct genotypes of SNPs in naive and primed hESCs were determined.

Abbreviations

FISH	Fluorescence in situ hybridization
FPKM	Fragments per kilobase of transcript per million mapped reads
H3K27Me3	Trimethylation of lysine 27 on histone 3
hESCs	Human embryonic stem cells
hiPSCs	Human induced pluripotent stem cells
hPSCs	Human pluripotent stem cells
HT	High expression of tdTomato
LT	Low expression of tdTomato
mEpiSCs	Mouse epiblast stem cells
mESCs	Mouse embryonic stem cells
PCA	Principal component analysis
PRC	Polycomb repressive complex
SG	Single GFP positive
SNP	Single-nucleotide polymorphism
ST	Single tdTomato positive
TG	TdTomato and GFP double positive
WT	Wildtype
XCI	X Chromosome inactivation

Supplementary Information

The online version contains supplementary material available at https://doi.org/10.1186/s12915-024-01994-y.

Additional file 1: Table S1-S4. Table S1. List of relevant biological reagents. Table S2. List of recipes of media. Table S3. List of recipes of buffer. Table S4. List of antibodies.

Acknowledgements

We thank our funders for the support.

Authors' contributions

Conceptualization: CA, WS; Methodology: SY, NW; Software: SY, NW; Data curation: SY, NW; Writing—original draft preparation: SY, CA, WS; Writing—review and editing: HW, CA, WS; Funding acquisition: WS, HW. All authors have read and agreed to the published version of the manuscript.

Funding

This research was supported by the National Natural Science Foundation of China (32001062 to W.S.), Beijing Institute for Stem Cell and Regenerative Medicine (2023FH106 to W.S.), National Key Research and Development Program of China (2018YFE0201102 to W.S., 2019YFA0110000 to H.W.) and National Natural Science Foundation of China (32200452 to A.C.R.)

Availability of data and materials
All data and materials are provided in the main text and the Additional files. Further raw data are available from the corresponding author upon request.

Declarations

Ethics approval and consent to participate
Not applicable.

Consent for publication
All authors approved the final manuscript and the submission to this journal.

Competing interests
The authors declare that they have no competing interests.

Author details
[1]Department of Obstetrics and Gynecology, Guangdong Provincial Key Laboratory for Major Obstetric Diseases, Guangdong Provincial Clinical Research Center for Obstetrics and Gynecology, Guangdong-Hong Kong-Macao Greater Bay Area Higher Education Joint Laboratory of Maternal-Fetal Medicine, The Third Affiliated Hospital, Guangzhou Medical University, Guangzhou, China. [2]State Key Laboratory of Stem Cell and Reproductive Biology, Institute of Zoology, Chinese Academy of Sciences, Beijing, China. [3]Institute for Stem Cell and Regeneration, Chinese Academy of Sciences, Beijing, China. [4]University of Chinese Academy of Sciences, Beijing, China. [5]Beijing Institute for Stem Cell and Regenerative Medicine, Beijing, China.

Received: 5 January 2024 Accepted: 28 August 2024
Published online: 18 September 2024

References

1. Deng X, Berletch JB, Nguyen DK, Disteche CM. X chromosome regulation: diverse patterns in development, tissues and disease. Nat Rev Genet. 2014;15(6):367–78.
2. Brockdorff N. Polycomb complexes in X chromosome inactivation. Philos Trans R Soc Lond B Biol Sci. 2017;372(1733):20170021.
3. Silva J, Mak W, Zvetkova I, Appanah R, Nesterova TB, Webster Z, et al. Establishment of Histone H3 Methylation on the Inactive X Chromosome Requires Transient Recruitment of Eed-Enx1 Polycomb Group Complexes. Dev Cell. 2003;4(4):481–95.
4. Plath K, Fang J, Mlynarczyk-Evans SK, Cao R, Worringer KA, Wang H, et al. Role of histone H3 lysine 27 methylation in X inactivation. Science. 2003;300(5616):131–5.
5. de Napoles M, Mermoud JE, Wakao R, Tang YA, Endoh M, Appanah R, et al. Polycomb group proteins Ring1A/B link ubiquitylation of histone H2A to heritable gene silencing and X inactivation. Dev Cell. 2004;7(5):663–76.
6. Almeida M, Pintacuda G, Masui O, Koseki Y, Gdula M, Cerase A, et al. PCGF3/5–PRC1 initiates Polycomb recruitment in X chromosome inactivation. Science. 2017;356(6342):1081–4.
7. Wang H, Wang L, Erdjument-Bromage H, Vidal M, Tempst P, Jones RS, et al. Role of histone H2A ubiquitination in Polycomb silencing. Nature. 2004;431(7010):873–8.
8. Gao Z, Zhang J, Bonasio R, Strino F, Sawai A, Parisi F, et al. PCGF Homologs, CBX Proteins, and RYBP Define Functionally Distinct PRC1 Family Complexes. Mol Cell. 2012;45(3):344–56.
9. Cao R, Wang L, Wang H, Xia L, Erdjument-Bromage H, Tempst P, et al. Role of histone H3 lysine 27 methylation in Polycomb-group silencing. Science. 2002;298(5595):1039–43.
10. Lessing D, Anguera MC, Lee JT. X chromosome inactivation and epigenetic responses to cellular reprogramming. Annu Rev Genomics Hum Genet. 2013;14:85–110.
11. Galupa R, Heard E. X-Chromosome Inactivation: A Crossroads Between Chromosome Architecture and Gene Regulation. Annu Rev Genet. 2018;52:535–66.
12. Namekawa SH, Payer B, Huynh KD, Jaenisch R, Lee JT. Two-step imprinted X inactivation: repeat versus genic silencing in the mouse. Mol Cell Biol. 2010;30(13):3187–205.
13. Lee JT, Bartolomei MS. X-inactivation, imprinting, and long noncoding RNAs in health and disease. Cell. 2013;152(6):1308–23.
14. Chen G, Schell JP, Benitez JA, Petropoulos S, Yilmaz M, Reinius B, et al. Single-cell analyses of X Chromosome inactivation dynamics and pluripotency during differentiation. Genome Res. 2016;26(10):1342–54.
15. Khan SA, Theunissen TW. Modeling X-chromosome inactivation and reactivation during human development. Curr Opin Genet Dev. 2023;82:102096.
16. Okamoto I, Patrat C, Thepot D, Peynot N, Fauque P, Daniel N, et al. Eutherian mammals use diverse strategies to initiate X-chromosome inactivation during development. Nature. 2011;472(7343):370–4.
17. Petropoulos S, Edsgard D, Reinius B, Deng Q, Panula SP, Codeluppi S, et al. Single-Cell RNA-Seq Reveals Lineage and X Chromosome Dynamics in Human Preimplantation Embryos. Cell. 2016;165(4):1012–26.
18. Patrat C, Ouimette JF, Rougeulle C. X chromosome inactivation in human development. Development. 2020;147(1)::dev183095.
19. Sahakyan A, Plath K, Rougeulle C. Regulation of X-chromosome dosage compensation in human: mechanisms and model systems. Philos Trans R Soc Lond B Biol Sci. 2017;372(1733):20160363.
20. Shen Y, Matsuno Y, Fouse SD, Rao N, Root S, Xu R, et al. X-inactivation in female human embryonic stem cells is in a nonrandom pattern and prone to epigenetic alterations. Proc Natl Acad Sci U S A. 2008;105(12):4709–14.
21. Silva SS, Rowntree RK, Mekhoubad S, Lee JT. X-chromosome inactivation and epigenetic fluidity in human embryonic stem cells. Proc Natl Acad Sci U S A. 2008;105(12):4820–5.
22. Bar S, Seaton LR, Weissbein U, Eldar-Geva T, Benvenisty N. Global Characterization of X Chromosome Inactivation in Human Pluripotent Stem Cells. Cell Rep. 2019;27(1):20-9 e3.
23. Vallot C, Ouimette JF, Makhlouf M, Feraud O, Pontis J, Come J, et al. Erosion of X Chromosome Inactivation in Human Pluripotent Cells Initiates with XACT Coating and Depends on a Specific Heterochromatin Landscape. Cell Stem Cell. 2015;16(5):533–46.
24. Patel S, Bonora G, Sahakyan A, Kim R, Chronis C, Langerman J, et al. Human embryonic stem cells do not change their X inactivation status during differentiation. Cell Rep. 2017;18(1):54–67.
25. Nazor KL, Altun G, Lynch C, Tran H, Harness JV, Slavin I, et al. Recurrent variations in DNA methylation in human pluripotent stem cells and their differentiated derivatives. Cell Stem Cell. 2012;10(5):620–34.
26. Khan SA, Park KM, Fischer LA, Dong C, Lungjangwa T, Jimenez M, et al. Probing the signaling requirements for naive human pluripotency by high-throughput chemical screening. Cell Rep. 2021;35(11):109233.
27. Bayerl J, Ayyash M, Shani T, Manor YS, Gafni O, Massarwa R, et al. Principles of signaling pathway modulation for enhancing human naive pluripotency induction. Cell Stem Cell. 2021;28:1549-1565.e12.
28. Bredenkamp N, Yang J, Clarke J, Stirparo GG, von Meyenn F, Dietmann S, et al. Wnt Inhibition Facilitates RNA-Mediated Reprogramming of Human Somatic Cells to Naive Pluripotency. Stem Cell Rep. 2019;13(6):1083–98.
29. Bredenkamp N, Stirparo GG, Nichols J, Smith A, Guo G. The Cell-Surface Marker Sushi Containing Domain 2 Facilitates Establishment of Human Naive Pluripotent Stem Cells. Stem Cell Rep. 2019;12(6):1212–22.
30. Chen H, Aksoy I, Gonnot F, Osteil P, Aubry M, Hamela C, et al. Reinforcement of STAT3 activity reprogrammes human embryonic stem cells to naive-like pluripotency. Nat Commun. 2015;6:7095.
31. Guo G, von Meyenn F, Santos F, Chen Y, Reik W, Bertone P, et al. Naive pluripotent stem cells derived directly from isolated cells of the human inner cell mass. Stem Cell Rep. 2016;6(4):437–46.
32. Qin H, Hejna M, Liu Y, Percharde M, Wossidlo M, Blouin L, et al. YAP Induces Human Naive Pluripotency. Cell Rep. 2016;14(10):2301–12.
33. Takashima Y, Guo G, Loos R, Nichols J, Ficz G, Krueger F, et al. Resetting transcription factor control circuitry toward ground-state pluripotency in human. Cell. 2014;158(6):1254–69.
34. Theunissen TW, Powell BE, Wang H, Mitalipova M, Faddah DA, Reddy J, et al. Systematic identification of culture conditions for induction and maintenance of naive human pluripotency. Cell Stem Cell. 2014;15(4):471–87.
35. Guo G, von Meyenn F, Rostovskaya M, Clarke J, Dietmann S, Baker D, et al. Epigenetic resetting of human pluripotency. Development. 2017;144(15):2748–63.

36. Sahakyan A, Kim R, Chronis C, Sabri S, Bonora G, Theunissen TW, et al. Human Naive Pluripotent Stem Cells Model X Chromosome Dampening and X Inactivation. Cell Stem Cell. 2017;20(1):87–101.
37. Vallot C, Patrat C, Collier AJ, Huret C, Casanova M, Liyakat Ali TM, et al. XACT Noncoding RNA Competes with XIST in the Control of X Chromosome Activity during Human Early Development. Cell Stem Cell. 2017;20(1):102–11.
38. Theunissen TW, Friedli M, He Y, Planet E, O'Neil RC, Markoulaki S, et al. Molecular Criteria for Defining the Naive Human Pluripotent State. Cell Stem Cell. 2016;19(4):502–15.
39. An C, Feng G, Zhang J, Cao S, Wang Y, Wang N, et al. Overcoming Autocrine FGF Signaling-Induced Heterogeneity in Naive Human ESCs Enables Modeling of Random X Chromosome Inactivation. Cell Stem Cell. 2020;27(3):482-97.e4.
40. Lengner CJ, Gimelbrant AA, Erwin JA, Cheng AW, Guenther MG, Welstead GG, et al. Derivation of pre-X inactivation human embryonic stem cells under physiological oxygen concentrations. Cell. 2010;141(5):872–83.
41. Kobayashi S, Hosoi Y, Shiura H, Yamagata K, Takahashi S, Fujihara Y, et al. Live imaging of X chromosome reactivation dynamics in early mouse development can discriminate naive from primed pluripotent stem cells. Development. 2016;143(16):2958–64.
42. Boroviak T, Nichols J. Primate embryogenesis predicts the hallmarks of human naïve pluripotency. Development. 2017;144(2):175–86.
43. Zhou F, Wang R, Yuan P, Ren Y, Mao Y, Li R, et al. Reconstituting the transcriptome and DNA methylome landscapes of human implantation. Nature. 2019;572(7771):660–4.
44. Erwin JA, Lee JT. Characterization of X-chromosome inactivation status in human pluripotent stem cells. Curr Protoc Stem Cell Biol. 2010;Chapter 1:Unit 1B.6.

Publisher's Note